

Article

Simulated Runoff and Sediment Yield Responses to Land-Use Change Using the SWAT Model in Northeast China

Limin Zhang ^{1,2}, Xianyong Meng ^{3,4,*} , Hao Wang ^{2,*} and Mingxiang Yang ^{2,*}

¹ College of Architecture and Civil Engineering, Beijing University of Technology (BJUT), Beijing 100124, China; zhanglm152@163.com

² State Key Laboratory of Simulation and Regulation of Water Cycle in River Basin & China Institute of Water Resources and Hydropower Research (IWHR), Beijing 100038, China

³ College of Resources and Environmental Science, China Agricultural University (CAU), Beijing 100094, China

⁴ Department of Civil Engineering, The University of Hong Kong (HKU), Pokfulam 999077, Hong Kong, China

* Correspondence: xymeng@cau.edu.cn or xymeng@hku.hk (X.M.); wanghao@iwhr.com (H.W.); yangmx@iwhr.com (M.Y.)

Received: 31 January 2019; Accepted: 27 April 2019; Published: 1 May 2019



Abstract: Land-use change is one key factor influencing the hydrological process. In this study, the Hun River Basin (HRB) (7919 km²), a typical alpine region with only four gauge meteorological stations, was selected as the study area. The China Meteorological Assimilation Driving Datasets for the SWAT model (CMADS), widely adopted in East Asia, was used with the Soil and Water Assessment Tool (SWAT) model to simulate runoff and sediment yield responses to land-use change and to examine the accuracy of CMADS in the HRB. The criteria values for daily/monthly runoff and monthly sediment yield simulations were satisfactory; however, the validation of daily sediment yield was poor. Forestland decreased sediment yield throughout the year, increased water percolation, and reduced runoff during the wet season, while it decreased water percolation and increased runoff during the dry season. The responses of grassland and forestland to runoff and sediment yield were similar, but the former was weaker than the latter in terms of soil and water conservation. Cropland (urban land) generally increased (increased) runoff and increased (decreased) sediment yield; however, a higher sediment yield could occur in urban land than that in cropland when precipitation was light.

Keywords: runoff; sediment yield; land-use change; SWAT; CMADS

1. Introduction

Water quantity and quality have become serious concerns in many countries around the world, negatively affecting the human survival environment and sustainable economic and social development [1–3]. Land-use and land-cover change (LUCC), one direct means for human activities (e.g., afforestation, deforestation, urbanisation, and reservoir construction) to alter the landscape, plays an important role in influencing the hydrologic response of watersheds in multiple ways [4,5]. LUCC is considered directly linked to changes in the hydrologic components in a watershed, such as evapotranspiration, surface runoff, groundwater, and stream flow, and hence can change flood frequency and severity, base flow, and annual mean discharge [6–9]. Following a conversion in land use, soil erosion will be altered in turn affecting the sediment yield [10–12]. Many previous studies throughout the world have shown that the changes in runoff and sediment yield are influenced by LUCC at different spatial and temporal scales [6–16]. For example, Buendia et al. [13] found that

increased forest area was the major driver of reduced stream flows and peak magnitudes as well as prevention of increases in sediment load in an upland Mediterranean catchment. Lin et al. [14] applied the Soil and Water Assessment Tool (SWAT) model to investigate runoff responses at annual, monthly, and daily time scales using the same meteorological input but two different land-use scenarios (1985 and 2006, with reduced forest and increased cropland and urbanized area); the results showed a varying change in runoff among the three time scales and three catchments in the Jinjiang catchment. Mueller et al. [15] investigated the impact of LUCC on sediment yield for a meso-scale catchment in the Southern Pyrenees and showed that LUCC had greater impacts on sediment yield than climate change. Most investigations have focused on the whole changes in runoff/sediment yield influenced by different historical land-use scenarios at annual scale; however, few studies regarding the impacts of individual land-use types on runoff and sediment at annual and seasonal scales have been conducted.

To evaluate the hydrologic and sediment effects of environmental change, several methods have been developed and are mainly divided into three categories: paired catchment approach, time series analysis (statistical method), and hydrological modelling [7,17]. The paired catchment approach is often considered to be the best method for the compensation of climatic variability in small experimental catchment during the observation period. However, it is typically carried out in small catchments because it is difficult to identify two medium- or large-sized catchments areas that are similar in area, shape, geology, climate, and vegetation [18,19]. The time series analysis method is a simple mathematical statistical model that cannot show the physical mechanism of a hydrological response. At the same time, owing to the complexity of factors affecting hydrological changes in the basin, it is easy to misjudge if other factors are excluded from the time series changes in the characteristic variables [20]. Among these approaches, the hydrological modelling method, particularly a physically based distributed hydrological model, is the most suitable for use in scenario studies and in assisting in understanding the mechanisms of influence resulting from land-use impacts [6,14]. Compared with other hydrological models, the SWAT model [21] is among the appropriate models for simulating runoff and sediment yield under different land-use scenarios and it has been widely used throughout the world (see SWAT Literature Database [22]). The SWAT model was used in this study because of its availability, convenience, friendly interface, and simple operation; it can be downloaded from the official website [23].

Spatial variabilities in precipitation and temperature are key factors in impacting the water balance of large watersheds, particularly in mountainous areas [21,24,25]. However, sediment yield is closely related to precipitation and runoff. Therefore, meteorological input data with high precision and quality aids in reducing the uncertainty in the model input and improves model simulation reliability. In this study, the SWAT model was driven by the China Meteorological Assimilation Driving Datasets for the SWAT model (CMADS) established by Dr. Xianyong Meng from China Agricultural University (CAU) [26]. The atmospheric re-analysis dataset CMADS was established by using Space-Time Multiscale Analysis System (STMAS) assimilation and big data technology that corrects the European Centre for Medium Range Weather Forecasts (ECMWF) with nearly 40,000 regional automatic stations in China such that it can better reflect the real surface meteorological conditions [27,28]. CMADS has formats suitable for SWAT, consisting of max/min temperature, precipitation, relative humidity, solar radiation, and wind speed and can drive the SWAT model without changing the data type. This is very convenient for users. Many researchers have shown the relatively higher accuracy of CMADS, which will provide important basic data for hydrological research in East Asia, especially in areas with scarce data [29–36]. For example, Liu et al. [29] applied CMADS, Climate Forecast System Reanalysis (CFSR), and observed meteorological data to the SWAT model and found that CMADS + SWAT obtained a better result than that of the other modes on the Qinghai–Tibet Plateau, northwest China, where meteorological stations are scarce. Compared with observed meteorological data (OBS) or CMADS, the SWAT model driven by OBS + CMADS provided the best simulation result for runoff in the Hailiutu River Basin [31]. Thom et al. [32] used rainfall data from the Tropical Rainfall Measuring Mission

(TRMM) and CMADS to simulate runoff of the Han River Basin on the Korean Peninsula and the accuracy was acceptable.

The Hun River basin (HRB) has a large population and is among the areas subject to serious water shortages in China. During recent years, the Chinese government has made a major strategic decision of ‘Revitalization of Old Industrial Bases in Northeast China’. Meanwhile, the Liaoning province government has proposed construction of the Shenfu Connection Area (Shenfu New Town) with an area of 605 km² to connect Shenyang and Fushun. Moreover, many studies have demonstrated that the government policies can have a considerable impact on land use, such as “Household Responsibility System” and “Grain to Green Program” [37,38]. In addition, in cold areas, the climate is characterized by a longer freezing period and winter every year. Therefore, it is essential to analyze the runoff and sediment yield under individual land-use types and it needs to be considered at a local scale.

The objectives of this study were to (1) calibrate and validate the SWAT model in terms of runoff and sediment yield based on CMADS in the HRB, (2) evaluate the impacts of individual land-use types on annual and seasonal runoff and sediment yield at a sub-basin scale; and (3) analyze the differences in runoff and sediment yield under individual land-use types during the wet and dry seasons.

2. Materials and Methods

2.1. Study Area

The total area of the HRB is 11,481 km² and the average annual runoff is approximately 3.05 billion m³. The study region (7919 km²) is upstream of Shenyang station (41°29′–42°16′ N, 123°22′–125°17′ E) within the HRB in Liaoning Province (Figure 1). The Dahuofang Reservoir is 18 km from Fushun and 68 km from Shenyang. The upstream of the reservoir is mountainous with elevations ranging from 400 to 800 m. The downstream of the reservoir is hills with the elevations of 100–200 m. The study region is affected by temperate semi-humid and semi-arid continental winds with an annual mean temperature of 4–8 °C. The area has a long and cold winter and a hot and rainy summer. Precipitation is mainly occurs during the period of June–September or May–August, accounting for 70%–80% of the total annual precipitation overall [39]. Grassland, cropland, and forestland are the dominant land-use types in the catchment.

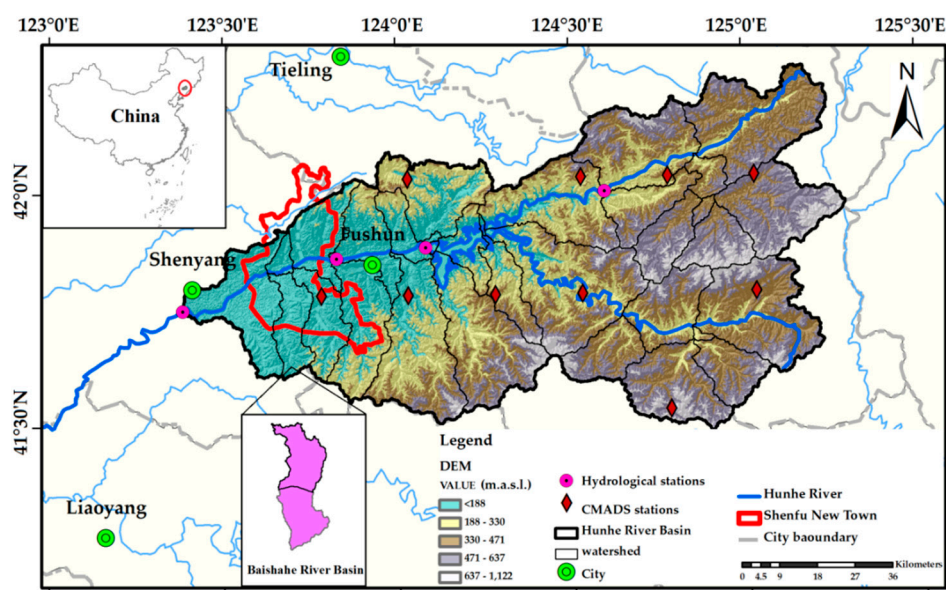


Figure 1. The range and location of the study region in China.

The Baishahe River is an important tributary in the Hun River downstream, and the main river flows to Shenfu New Town (SNT) [40]. The Baishahe River Basin (BRB) covers an area of 162.41 km²;

the overlap area of BRB and SNT is 85.85 km². Analyzing the changes in land use in SNT from 1997 to 2011, we found that the conversion of land use was mainly among forestland, cropland, grassland, and residential land, such as returning cropland to forestland and/or residential land. SNT is a developing city, the land-use conversion of which could be a representative of urban expansion in China.

2.2. Data Collection

The spatial data used in this study included digital elevation model (DEM), soil type, and land-use data. The 90 m × 90 m resolution DEM was derived from CGIAR—Consortium for Spatial Information (CGIAR-CSI) [41]. The soil data set was provided by the Environmental and Ecological Science Data Center for West China, National Natural Science Foundation of China [42]. The Chinese soil dataset (v1.1) was based on the Harmonized World Soil Database (HWSD) at a scale of 1:1,000,000 and a resolution of 1 km [43]. The percentages of the total area of the seven soil types in the basin are as follows: Calcaric Cambisols: 0.13%, Haplic Phaeozems: 17.59%, Cumulic Anthrosols: 4.67%, Haplic Luvisols: 56.61%, Gleyic Luvisols: 18.30%, Urban: 1.67%, and water bodies: 0.96%. Soil water characteristics for each soil type were obtained by using the SPAW (Soil-Plant-Air-Water) computer model developed by the U.S. Department of Agriculture (USDA) [44]. The land-cover map was drawn using the global land cover for the year 2000 (GLC 2000) project coordinated by the Global Vegetation Monitoring Unit of the European Commission Joint Research Centre with a resolution of 1 km, as loaded from <http://westdc.westgis.ac.cn> [45]. The land-use types were classified into five categories according to the SWAT code. The land-use types and their distribution in the HRB are shown in Figure 2. The percentages of the total area of different land-use types in the basin are as follows: Agricultural Land-Generic (AGRL): 16.59%, Forest-Mixed (FRST): 79.17%, Pasture (PAST): 3.76%, Residential-High Density (URHD): 0.39%, and Water (WATR): 0.09%. The BRB, whose sub-basin number is 22 in this study, was selected to investigate the impacts of individual land-use types on runoff and sediment yield. Its main land use types are forest land (42.0 km², 31.1%) and cropland (120.41 km², 68.9%) with the land-use data of GLC2000 and its main soil types are Cumulic Anthrosols (18.82%), Haplic Luvisols (47.99%), and Haplic Phaeozems (33.54%).

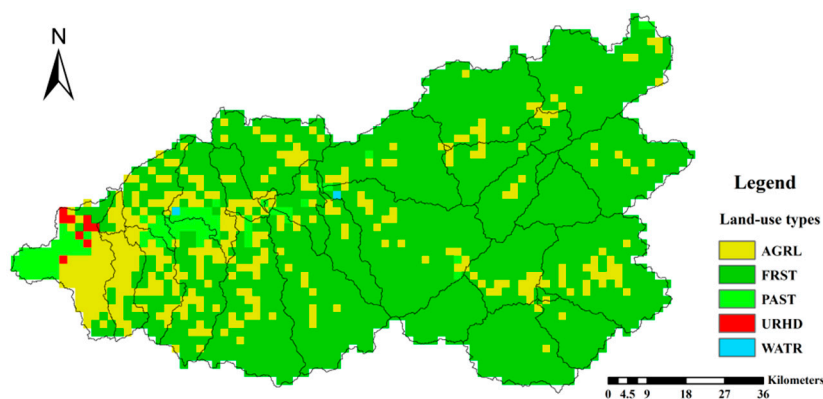


Figure 2. The land use types and their distribution in the HRB. Remarks: FRST—Forestland; PAST—Grassland; AGRL—Cropland; URHD—Urban land; and WATR—Water.

Meteorological data including daily precipitation, maximum and minimum air temperature, relative humidity, wind speed, and solar radiation were obtained from the CMADS official website (<http://www.cmads.org/>) [26]. The spatial resolution of CMADS1.1 is 1/4° and the period is 2008–2016. The observed runoff (unit: m³/s) and sediment data (unit: kg/s) at Beikouqian, Dahuofang Reservoir (no sediment yield data), Fushun, and Shenyang gauge stations between 2008 and 2014 were derived from the Annual Hydrological Report of the People’s Republic of China published by the Ministry of Water Resources of the People’s Republic of China.

2.3. Methods

2.3.1. Hydrological Modelling

The SWAT model developed by Jeffrey G. Arnold is a continuous-time, semi-distributed, and process-based river basin model [46]. It is a physically based model operating on a daily time step and was initially developed to predict the impact of management on water, sediment, and agriculture chemical yields [47]. SWAT is a deterministic model, which means that each successive model run using the same inputs will result in the same outputs. Therefore, this type of model is suitable to separate and evaluate the effects of a single variable, and it is easy to compare the relative effects from one to another [48]. In applying the SWAT model, the study area is first divided into sub-basins based on the DEM, and then these are further divided into one or more hydrologic response units (HRUs). Each HRU, consisting of unique land use, management, topographical, and soil characteristics, is an independent unit of the SWAT model and does not interact with the other HRUs. Simulation of the watershed hydrology is separated into a land phase, which controls the amount of water, sediment, nutrient, and pesticide loadings to the main channel in each sub-basin, and an in-stream or routing phase, which is the movement of water, sediment, etc., through the channel network of the watershed to the outlet [46]. The SWAT model is based on the water balance in the soil profile, and the processes simulated include infiltration, surface runoff, evapotranspiration (ET), lateral flow, and percolation. All the water balance processes in the same HRU are regarded as being consistent.

The study area was divided into 34 sub-basins and 317 HRUs. The Soil Conservation Service (SCS) curve method [49] was used to calculate the surface runoff generated by each independent HRU resulting from the daily input precipitation; the confluence was eventually obtained in the exit section. The Penman–Monteith method [50] was used to calculate the potential evapotranspiration in the study area and the variable storage routing method developed by Williams (1969) [51] was selected to calculate the water evolution in the main channel. Soil erosion was computed using the Modified Universal Soil Loss Equation (MUSLE) [52]. Sediment loadings from each HRU in the landscape were then summed at the sub-basin level and the resulting loads were routed by runoff and distributed to the watershed outlet [53]. Sediment transport in the channel network was simultaneously controlled by deposition and degradation processes, which depended on the sediment loads originating from upland areas and the channel transport capacity [53]. A more detailed description of the mechanisms and structure of the SWAT model can be found in the theoretical documentation [23] and in Arnold et al. [21].

2.3.2. SWAT Calibration, Validation and Performance Evaluation

The SWAT Calibration Uncertainty Program (SWAT-CUP) was selected for the sensitivity analysis, calibration, and validation. SUFI-2 (Sequential Uncertainty Fitting) is a comprehensive optimization and gradient search method able to simultaneously calibrate multiple parameters and with a global search function. It also considers the uncertainty of the input data, model parameters, and model structure [54,55].

The calibration and validation of runoff and sediment were completed at monthly and daily scales at the gauge stations in the HRB. The calibration period was 2008–2012 encompassing average, wet, and dry years and the validation period was 2013–2014. Model performance, defined as the goodness of fit between observed and predicted runoff/sediment yield, was quantitatively evaluated using the Nash–Sutcliffe efficiency coefficient (NSE), the coefficient of determination (R^2), and percent bias (PBIAS) [56]. R^2 ranges from 0 to 1; and typically values greater than 0.5 are considered acceptable [57,58]. When NSE and PBIAS are consistent with the given criteria proposed by Moriasi et al. [56] ($NSE > 0.5$; $\pm 15\% \leq PBIAS < \pm 25\%$ for runoff; and $\pm 30\% \leq PBIAS < \pm 55\%$ for sediment yield) for a monthly time step, the model is considered to be applicable to the catchment and the impact analyses.

2.3.3. Data Simulation

In this study, data simulation was based on four land-use and three precipitation scenarios. We assumed four land-use scenarios (forestland, grassland, cropland, and urban land, respectively) in extreme cases throughout the whole SNT region and as a part of land use within the HRB in each model run. Calibrated parameters were used and the simulation period was set as 2008 to 2012 every time using the same climatic forcing data because of the serious debris flow that occurred during 2013. The land-use condition of GLC2000 in SNT was set as the baseline scenario. Then, we assessed the contribution of changes in individual land-use types on runoff and sediment in the selected sub-basin (BRB) at annual and seasonal scales. Under Scenario 1 (S1), SNT was covered only by forestland, referring to the conversion of cropland to forestland in the BRB. Under Scenario 2 (S2), SNT was covered only by grassland, transforming forestland and cropland into grassland in the BRB. Under Scenario 3 (S3), SNT was covered only by cropland, assuming a change from forestland into cropland in the BRB. Scenario 4 (S4), SNT was covered only by urban land, converting forestland and cropland into urban land in the BRB. The information of land-use scenarios were shown Figure 3 and Table 1. Under the different scenarios, the land-use change in the BRB (as shown in Figure 3) only occurred in the overlap area of the BRB and SNT, and the land use of other areas and the meteorological inputs remained constant; therefore, it was easy to distinguish the contribution of changes in individual land-use types on runoff and sediment yield.

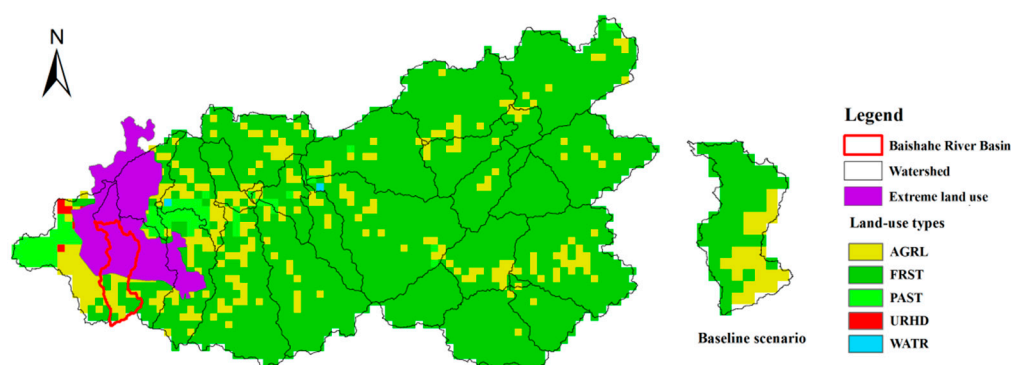


Figure 3. Land-use change scenarios in the BRB in the HRB. “Extreme land use” means the land-use types are FRST, PAST, AGRL, and URHD under S1, S2, S3, and S4, respectively. Remarks: FRST—Forestland; PAST—Grassland; AGRL—Cropland; URHD—Urban land; and WATR—Water.

Table 1. Land-use types under different scenarios in the BRB.

Scenarios	LUCC Description in BRB	Forestland		Grassland		Cropland		Urban	
		Area (km ²)	%						
Baseline	GLC2000 (forestland and cropland)	42	25.86	—	—	120.41	74.14	—	—
S1	Cropland changed into forestland	118.1	72.72	—	—	44.31	27.28	—	—
S2	Forestland and cropland changed into grassland	32.25	19.86	85.85	52.86	44.31	27.28	—	—
S3	Forestland changed into cropland	32.25	19.86	—	—	130.16	80.14	—	—
S4	Forestland and cropland changed into urban land	32.25	19.86	—	—	44.31	27.28	85.85	52.86

To further research the responses of runoff and sediment yield to land-use change, three main time scales (annual and wet and dry seasons) were adopted in this study. The wet season was further divided into wet season 1 (W1) and wet season 2 (W2) and the dry season was divided into dry season 1 (D1) and dry season 2 (D2). W1 was from May to September, and correspondingly, D1 was October to April. W2 ranged from June to September while D2 was October to May.

3. Results

3.1. Model Calibration and Validation

The calibrated parameters with their initial values and descriptions are presented in Table 2. The model results for calibration and validation based on performance criteria in the present study are listed in Table 3. The runoff and sediment yield for the calibration and validation at the gauge stations between simulated and observed data in the HRB are shown in Figures 4–7 and Table 3.

Table 2. Parameters used to calibrate runoff and sediment yield in the HRB.

Parameter	Definition	Min. Value	Max. Value
Parameters used to calibrate runoff			
ALPHA_BNK	Baseflow alpha factor for bank storage	0	1
CN2	SCS runoff curve number for moisture condition II	35	98
SOL_K	Soil conductivity	0	2000
CH_K2	Effective hydraulic conductivity in the main channel	0	150
SOL_BD	Soil bulk density	1.1	1.9
GWQMN	Threshold depth of water in the shallow aquifer required for return flow to occur	0	500
GW_REVAP	Groundwater “revap” coefficient	0.02	0.2
ESCO	Soil evaporation compensation factor	0.01	1
CH_N2	Manning’s n value for main channel	0	0.3
GW_DELAY	Groundwater delay time	0	500
SOL_AWC	Soil available water storage capacity	0	1
ALPHA_BF	Baseflow alpha factor	0	1
SFTMP	Snowfall temperature	−5	5
SMTMP	Snow melt base temperature	−5	5
Parameters used to calibrate sediment yield			
SPCON	Linear parameters for calculating the channel sediment routing	0.001	0.01
SPEXP	Exponent parameter for calculating the channel sediment routing	1	1.5
CH_COV	Channel cover factor	0	1
CH_EROD	Channel erodibility factor	0	0.6
PRF	Peak rate adjustment factor for sediment routing in the main channel	0	2
USLE_K	USLE equation soil erodibility (K) factor	0	0.65

Table 3. Criteria for examining model calibration and validation accuracy.

Time Scales	C/V	Criteria	Runoff				Sediment		
			Beikouqian	Dahuofang Reservoir	Fushun	Shenyang	Beikouqian	Fushun	Shenyang
Monthly	Calibration (2008–2012)	NSE	0.92	0.78	0.82	0.83	0.56	0.93	0.95
		R ²	0.94	0.8	0.82	0.84	0.57	0.96	0.96
		PBIAS (%)	19.56	21.62	13.02	15.12	27.54	7.92	23.84
	Validation (2013–2014)	NSE	0.89	0.67	0.7	0.75	0.002	0.41	0.84
		R ²	0.94	0.69	0.74	0.7	0.99	0.96	0.9
		PBIAS (%)	16.75	18.11	22.81	23.72	97.4	68.9	41.1
Validation (2014)	NSE					0.62	0.65	0.72	
	R ²					0.68	0.71	0.8	
	PBIAS (%)					11.86	22.16	32.9	
Daily	Calibration (2008–2012)	NSE	0.79	0.53	0.64	0.65	0.29	0.4	0.53
		R ²	0.8	0.55	0.65	0.67	0.5	0.47	0.57
		PBIAS (%)	11.14	24.52	25.3	24.84	60.68	25.77	16.98
	Validation (2013–2014)	NSE	0.85	0.56	0.57	0.67	0.12	0.36	0.44
		R ²	0.86	0.63	0.66	0.69	0.94	0.85	0.67
		PBIAS (%)	1.44	20.72	11.6	11.5	91.96	41.52	5.56

Note: “C/V” means “Calibration/Validation”.

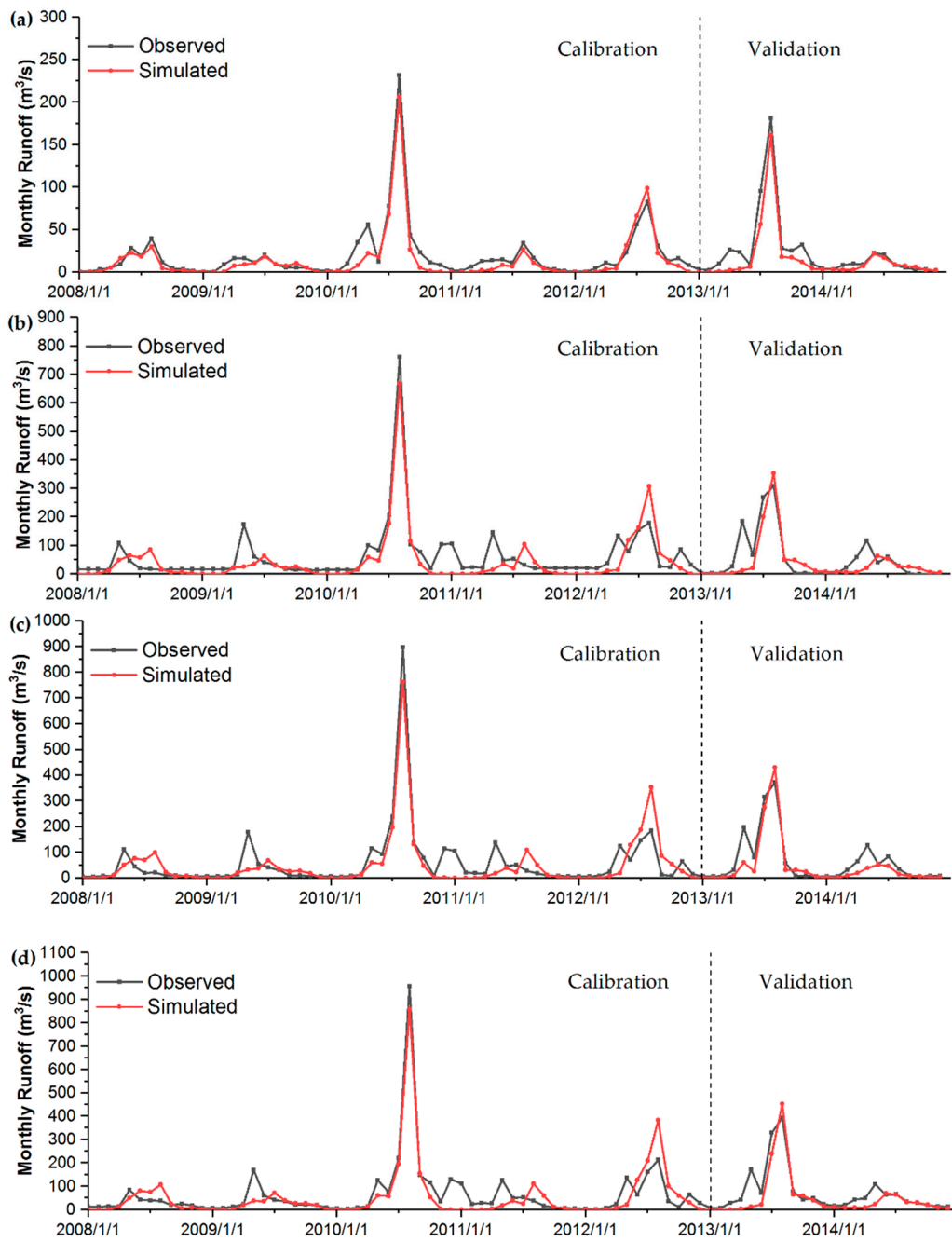


Figure 4. Comparison of observed and simulated monthly runoff during the calibration (2008–2012) and validation periods (2013–2014): (a) Beikouqian, (b) Dahuofang Reservoir, (c) Fushun, and (d) Shenyang.

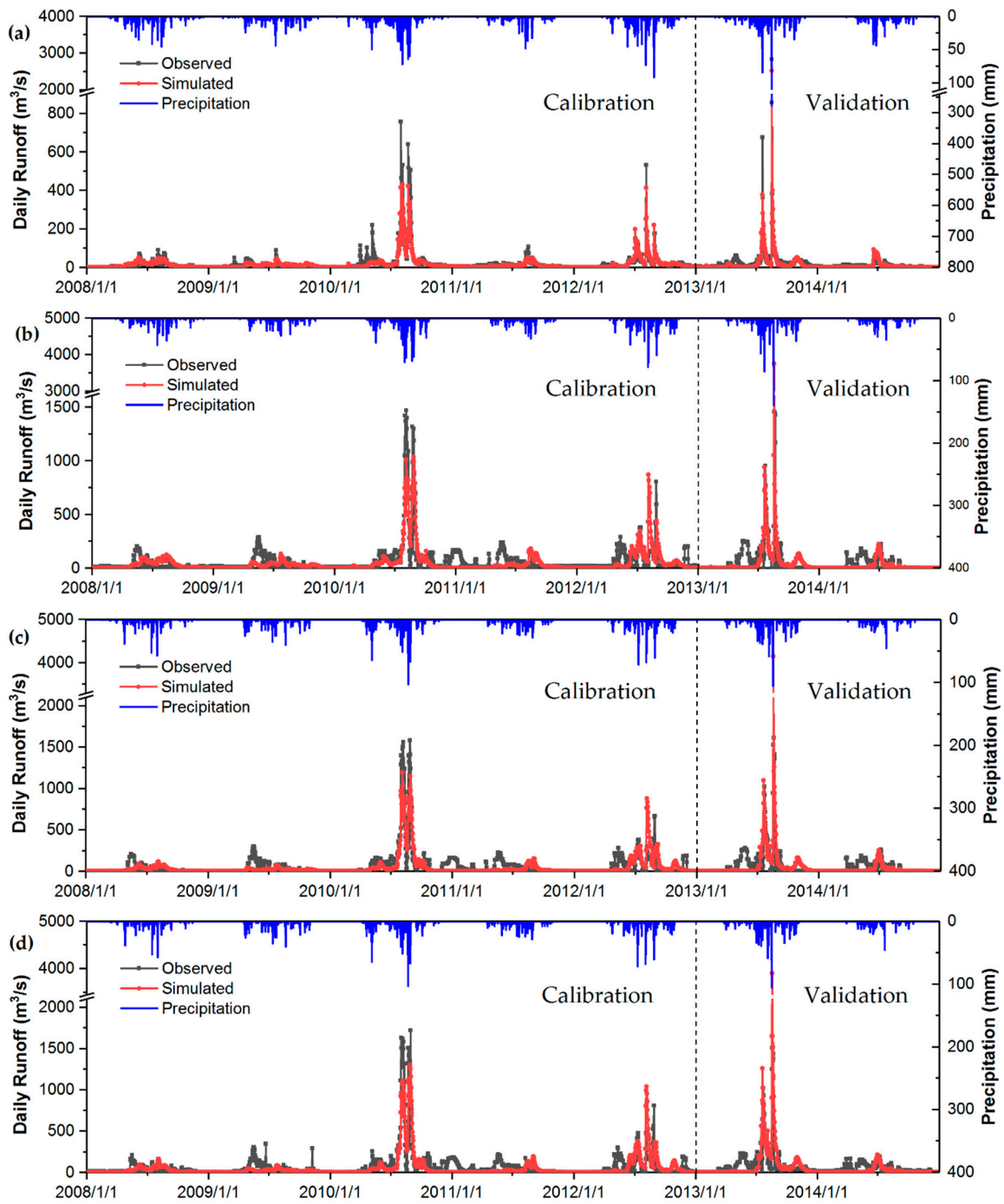


Figure 5. Comparison of observed and simulated daily runoff during the calibration (2008–2012) and validation periods (2013–2014): (a) Beikouqian, (b) Dahuofang Reservoir, (c) Fushun, and (d) Shenyang.

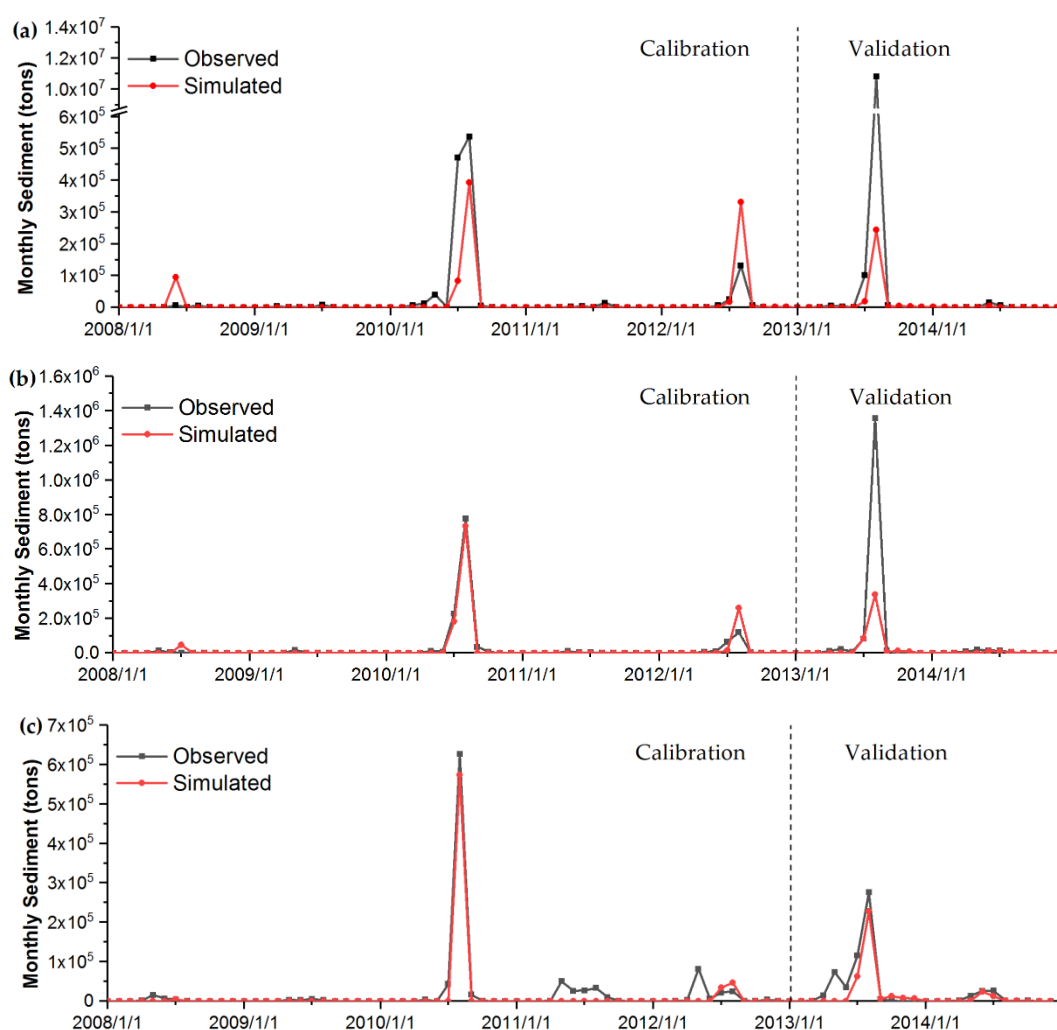


Figure 6. Comparison of observed and simulated monthly sediment yield during the calibration (2008–2012) and validation periods (2013–2014): (a) Beikouqian, (b) Fushun, and (c) Shenyang.

For monthly and daily runoff, all the NSE and R^2 values were greater than 0.5 and the PBIAS values were within a range of $\pm 25\%$, suggesting satisfactory simulation was achieved according to Moriasi et al. [52].

For monthly sediment, the calibration result was satisfied; however, the validation result was poor for the Beikouqian and Fushun stations, particularly for the upstream Beikouqian station (the NSE and R^2 were 0.002 and 0.99, respectively). The total observed sediment yield during August 2013 was approximately 1.08 million tons; however, the simulated was only 0.24 million tons, 0.84 million tons lower than the observed (Figure 6). The maximum daily average sediment transport rate was 94 tons per second, i.e., 8,121,600 tons per day, observed at Beikouqian station on 17 August 2013. According to the 2013 Bulletin of Flood and Drought Disaster in China [59] published on the internet by the Ministry of Water Resources of the People's Republic of China, a heavy rainstorm occurred north of Liaoning Province from 15–17 August 2013, and the maximum point of rainfall accumulation (456 mm) was observed at Hongtoushan Station, Fushun, Liaoning Province. The upstream Hun River was subject to an extraordinary 50-year flood leading to a large-scale debris-flow-dominated geohydrological process [60]. This debris flow disaster might have resulted in a considerable increase in sediment and resulting in the poor evaluation during the validation period (2013–2014). At the same time, a similar reason or more complex factors led to a disappointing result (most NSE values were lower than 0.5) for daily sediment during the calibration and validation periods, particularly for the upstream and middle stream hydrological stations.

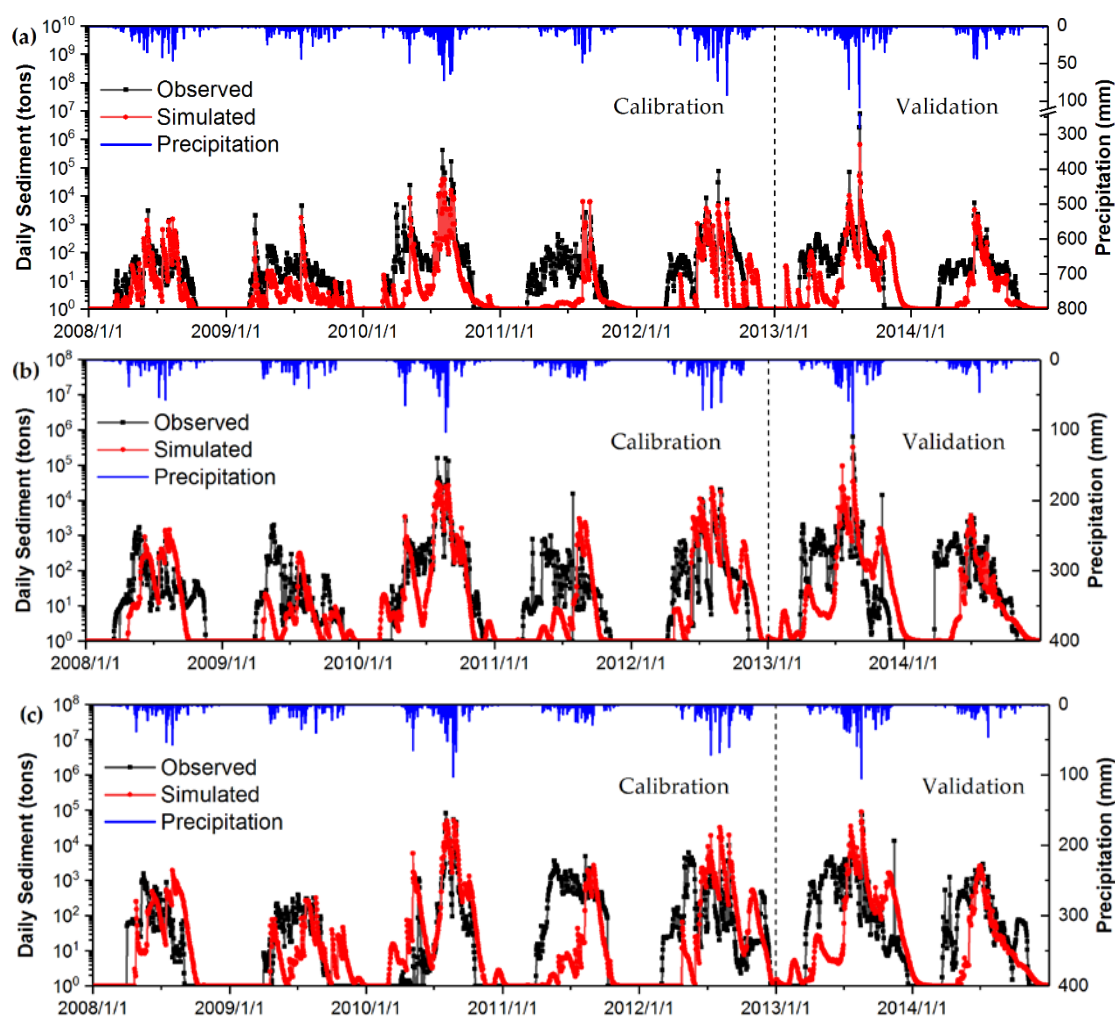


Figure 7. Comparison of observed and simulated daily sediment yield during the calibration (2008–2012) and validation periods (2013–2014): (a) Beikouqian, (b) Fushun, and (c) Shenyang.

In practice, the model performance was good during both calibration and validation for runoff, particularly for the upstream region of the HRB. The cause of the difference in consistency of the simulation hydrographs among the gauge stations may be related with the human activities (e.g., irrigation, reservoir operation, and water diversion), which can greatly affect hydrological processes [48,61]. In this study the upstream is a reservoir water source protection region with a larger area of forestland and fewer external factors; in contrast, two big cities (Fushun and Shenyang) and considerable cropland occur in the downstream of the HRB. This is a probable reason why the simulated flood peak was higher than the observed at Dahuofang Reservoir, Fushun, and Shenyang stations on 17 August 2013 (as shown in Figure 5b–d).

If the validation for the monthly sediment yield were to be changed to 2014, all the indicator values met the requirements (Table 3). Therefore, the SWAT model was thought to be a reliable representation of hydrologic processes and sediment export and can be used to simulate responses for the studied catchment at a monthly scale.

3.2. Water Balance Components Under Different Land-Use Scenarios

To further analyze the impacts of LUCC changes on the hydrological cycle, the hydrological components of individual land-use scenarios were assessed based on model simulation. The analysis results showed that the water balance varied among different land-use scenarios at different time scales in the BRB (Figure 8).

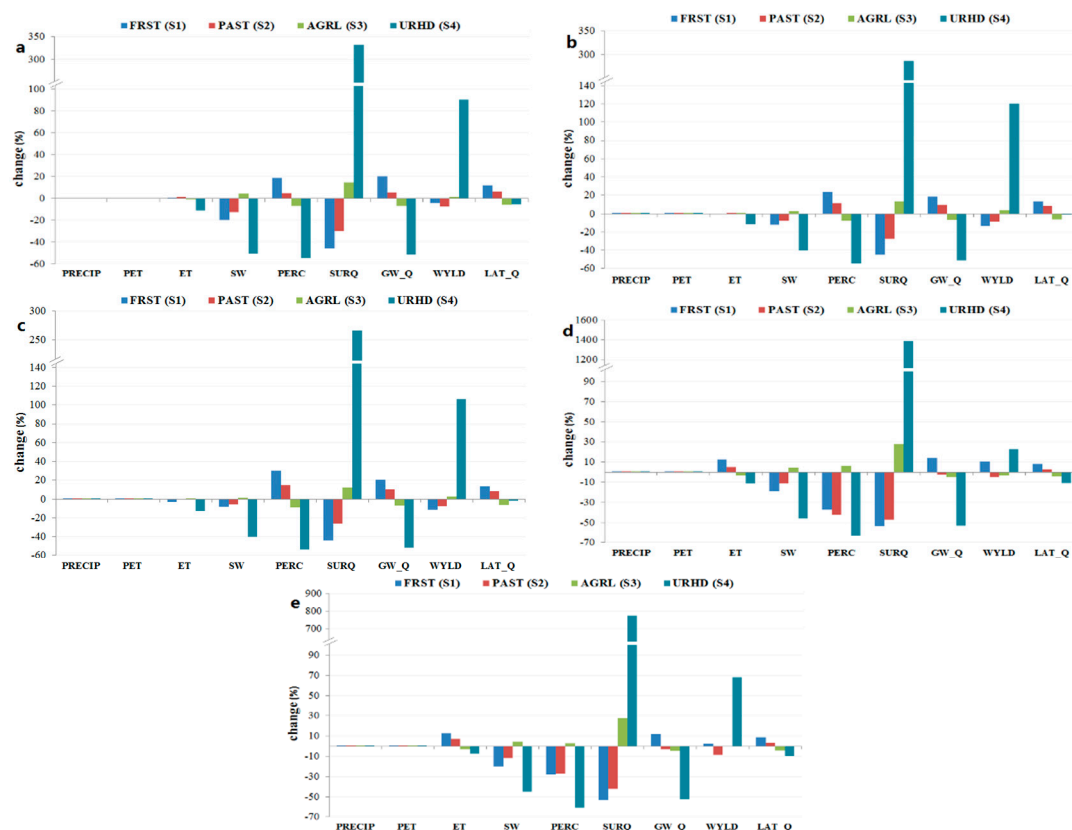


Figure 8. Impact of land-use change on water balance components at all statistical time scales: (a) refers to “annual” scale; (b) refers to “W1”; (c) refers to “W2”; (d) refers to “D1”; and (e) refers to “D2”. FRST—Forestland; PAST—Grassland; AGRL—Cropland; URHD—Urban land.

The impact of land-use change on the annual water balance components is shown in Figure 8a. Under the four hypothetical land-use change scenarios applied in our study sub-basin (the BRB), when the baseline land use (consisting of cropland and forestland) was converted to cropland/urban land, or to grassland/forestland, this would lead to the same change trend of the water balance components, excluding soil water content. For example, when changing the baseline scenario to the urban land scenario, the amount of water percolation (PERC) decreased 54.22% (2.66 mm), groundwater discharge (GW_Q) decreased by 51.32% (2.14 mm), soil water content (SW) decreased by 50.15% (17.02 mm), surface runoff (SURQ) increased by 332.27% (8.76 mm), and water yield (WYLD) increased 90.31% (6.61 mm). However, when by changing the baseline scenario to the forestland scenario, PERC and GW_Q increased by 18.77% and 20.03% (1.18 mm and 0.76 mm), respectively, and SW, SURQ, and WYLD decreased by 19.72%, 45.83%, and 4.29% (5.05 mm, 1.33 mm, and 0.55 mm), respectively. Other water balance components (e.g., precipitation (PRECIP), potential evapotranspiration (PET), actual evapotranspiration (ET)) insignificantly changed, except for a 10.75% reduction in ET under urban land scenario.

During the wet season (W1 and W2), the change trend of the water balance components (Figure 8b,c) was similar to that at annual scale.

During the dry season (D1 and D2), the changes in the water balance components influenced by land-use change scenarios were consistent (Figure 8d,e). For D1, the forestland scenario (S1) increased ET, GW_Q, and WYLD by 12.45%, 14.00%, and 10.32% (1.45 mm, 0.34 mm, and 0.27 mm), respectively, and decreased SW, PERC, and SURQ by 18.79%, 37.40%, and 53.62% (6.50 mm, 0.32 mm, and 0.07 mm), respectively. The urban land scenario (S4) decreased ET, SW, PERC, and GW_Q by 11.51%, 45.94%, 63.20%, and 53.00% (1.34 mm, 15.89 mm, 0.54 mm, and 1.29 mm), respectively, and increased SURQ and WYLD by 1385.94% and 23.04% (1.90 mm and 0.61 mm), respectively. There were few water

balance components that changed more than 5% under the grassland (S2) and cropland scenarios (S3). The grassland scenario (S2) resulted in a decrease in SW, PERC, and SURQ of 11.17%, 42.19%, and 47.38% (3.86 mm, 0.36 mm, and 0.07 mm), respectively. Cropland scenario (S3) increased PERC and SURQ by 6.21% and 27.76% (0.05 mm and 0.04 mm), respectively. Therefore, during the dry season, forestland and urban land have a great effect on the water balance components.

3.3. Contribution of Changes in Individual Land-Use Scenarios on Runoff

Simulated runoff changes resulting from the land-use change scenarios at different time scales under the same meteorological inputs (2008–2012) are summarized and compared in Table 4.

(1) Annual scale

The impact of land-use change on annual runoff is shown in Figure 9 and Table 4. The urban land scenario (S4) dramatically increased runoff by 90.23% ($0.62 \text{ m}^3/\text{s}$), followed by the cropland scenario (S3) with a minor increase in runoff (1.08%). However, the scenarios of forestland (S1) and grassland (S2), respectively, reduced runoff by 4.05% and 7.27% ($0.03 \text{ m}^3/\text{s}$ and $0.05 \text{ m}^3/\text{s}$). Meanwhile, when compared with forestland, grassland plays an important role in reducing runoff at annual scale. The contribution of changes in individual land-use scenarios on runoff at annual scale was urban land > cropland > baseline > forestland > grassland.

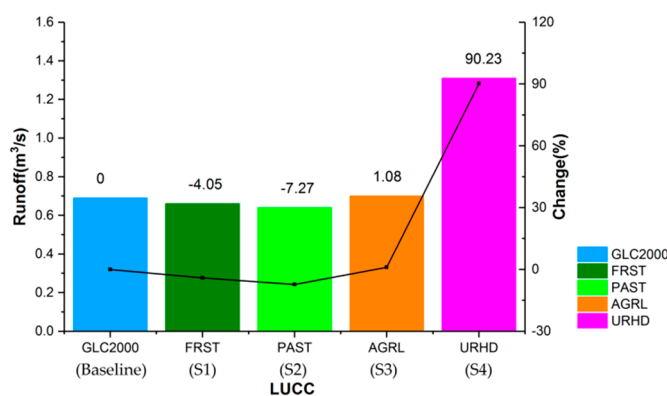


Figure 9. Responses of different land-use scenarios to annual runoff. Remarks: FRST—Forestland; PAST—Grassland; AGRL—Cropland; URHD—Urban land.

Moreover, at annual scale, the coefficients of determination ($n = 12$) at the sub-basin scale under the scenarios of urban land, cropland, baseline, grassland, and forestland, were 0.87, 0.41, 0.36, 0.25, and 0.15, respectively. The high R^2 for the rainfall–runoff relationship under the urban land scenario suggests that changes in runoff in the sub-basin under this scenario (covered by a large area of impervious surface) were actually mainly a function of the changes in precipitation, while the weakest rainfall–runoff relationship occurred under the forestland scenario (Figure 10).

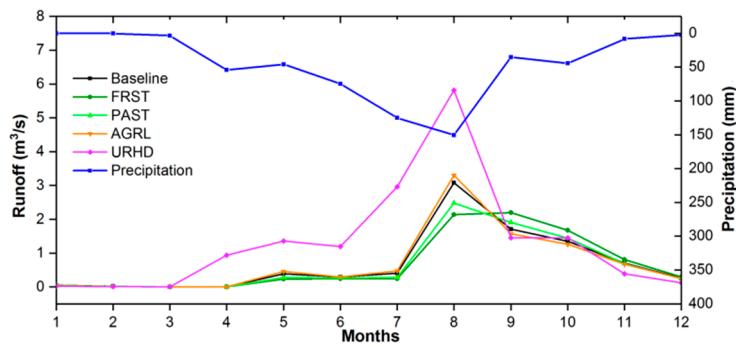


Figure 10. Responses of different land-use scenarios to average monthly runoff. Remarks: FRST—Forestland; PAST—Grassland; AGRL—Cropland; URHD—Urban land.

(2) Wet season and dry season

The contribution of changes on runoff during the wet seasons (W1 and W2) under different scenarios was similar to that at annual scale (Figures 9 and 11). In addition, the scenarios of urban land (S4) and cropland (S3) increased runoff (from 90.23% to 117.5% and from 1.08% to 3.87%, respectively) while forestland (S1) and grassland (S2) reduced runoff (from −4.05% to −13.83% and from −7.27% to −11.27%, respectively), compared with the values at annual scale (Table 4). For example, the urban land scenario (S4) increased runoff by 117.5% (1.382 m³/s) and the forestland scenario (S1) decreased runoff by 13.83% (0.163 m³/s) during W1. Reviewing Figure 11 and Table 4, we found that the range of the change rate of runoff was influenced by individual land-use scenarios during W2 less than that during W1. The reason might be that the differences among the effects of land-use change on runoff decrease if the denominator runoff (or precipitation) increases during wet season (Figure 11a,b). The contribution of changes in individual land-use scenarios on runoff during the wet season was urban land > cropland > baseline > grassland > forestland.

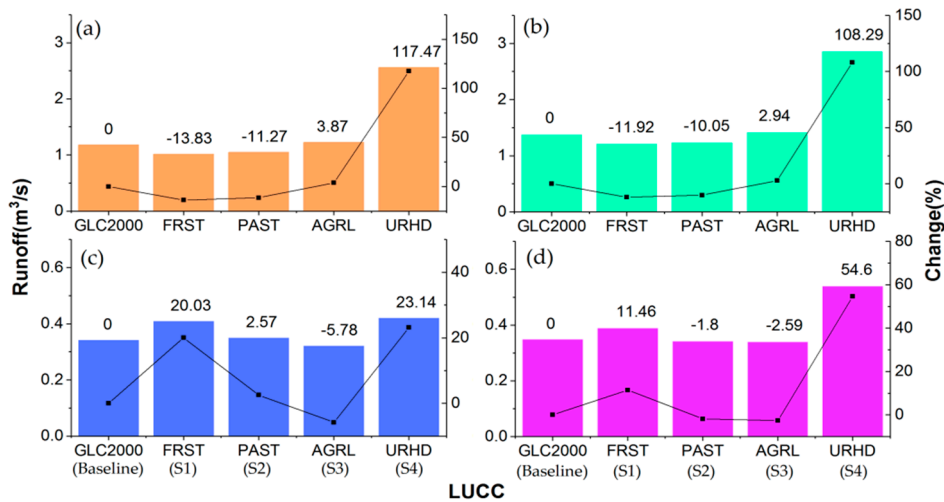


Figure 11. Runoff responses of different land-use scenarios during the wet season (W1 and W2) and dry season (D1 and D2): (a) refers to “W1”; (b) refers to “W2”; (c) refers to “D1”; and (d) refers to “D2”. FRST—Forestland; PAST—Grassland; AGRL—Cropland; URHD—Urban land.

Table 4. Simulated runoff changes resulting from the land-use change scenarios at different time scales.

Time Scales	Average Monthly Precipitation (mm)	Land-Use Scenarios									
		GLC2000 (Baseline)		FRST (S1)		PAST (S2)		AGRL (S3)		URHD (S4)	
		Q (m ³ /s)	R (%)	Q (m ³ /s)	R (%)	Q (m ³ /s)	R (%)	Q (m ³ /s)	R (%)	Q (m ³ /s)	R (%)
D1	16.2	0.341	—	0.409	20.03	0.35	2.57	0.321	−5.78	0.42	23.14
D2	19.9	0.348	—	0.388	11.46	0.341	−1.8	0.339	−2.59	0.538	54.6
Annual	45.38	0.69	—	0.66	−4.05	0.64	−7.27	0.7	1.08	1.31	90.23
W1	86.3	1.176	—	1.013	−13.83	1.044	−11.27	1.222	3.87	2.558	117.5
W2	96.4	1.372	—	1.208	−11.92	1.234	−10.05	1.412	2.94	2.857	108.3
D1–D2	3.7	0.007	—	−0.021	−8.57	−0.009	−4.37	0.018	3.19	0.118	31.46
W1–W2	10.1	0.196	—	0.195	1.91	0.19	1.22	0.19	−0.93	0.299	−9.18

Note: “W1–W2” means variable change from W1 to W2; and similarly for “D1–D2”. FRST—Forestland; PAST—Grassland; AGRL—Cropland; URHD—Urban land.

Table 4 and Figure 11c,d show that in contrast to the responses of runoff to land use change at annual and wet seasonal scales, the forestland scenario (S1) increased runoff by 20.03% and 11.46% (0.068 m³/s and 0.04 m³/s) during D1 and D2, respectively, while the cropland scenario (S3) decreased runoff by 5.78% and 2.59% (0.02 m³/s and 0.01 m³/s) during D1 and D2, respectively. Moreover, during D1 and D2, the urban land scenario (S4) increased runoff by a relatively moderate amount (23.14% (0.079 m³/s) and 54.60% (0.19 m³/s), respectively) compared with the sharp contrast at annual and wet seasonal scales (all were greater than 90% (0.62 m³/s)). Nevertheless, when the baseline land use (consisting of cropland and forestland) was converted to grassland, the effects of land-use change on runoff were opposite in the D1 and D2 (Table 4). The grassland scenario (S2) increased 2.57% (0.009 m³/s) of runoff during D1 but reduced runoff by 1.80% (0.007 m³/s) during D2. The contribution of changes in individual land-use scenarios on runoff during D1 and D2 were urban land > forestland > grassland > baseline > cropland; and urban land > forestland > baseline > grassland > cropland, respectively.

3.4. Contribution of Changes in Individual Land-Use Scenarios on Sediment Yield

Simulated sediment yield changes resulting from the land-use change scenarios at different time scales were summarized and compared as listed in Table 5.

Table 5. Simulated sediment yield changes resulting from land-use change scenarios at different time scales.

Time Scales	Average Monthly Precipitation (mm)	Land-Use Scenarios									
		GLC2000 (Baseline)		FRST (S1)		PAST (S2)		AGRL (S3)		URHD (S4)	
		S (tons)	R (%)	S (tons)	R (%)	S (tons)	R (%)	S (tons)	R (%)	S (tons)	R (%)
D1	16.2	4.73	—	1.47	−68.99	1.47	−68.83	7.25	53.29	11.31	139.32
D2	19.9	25.34	—	7.69	−69.65	7.75	−69.42	38.82	53.22	17.82	−29.68
Annual	45.38	122.8	—	33.23	−72.94	33.64	−72.61	184.16	49.97	43.11	−64.89
W1	86.3	288.1	—	77.69	−73.03	78.68	−72.69	431.83	49.89	87.63	−69.58
W2	96.4	317.73	—	84.3	−73.47	85.43	−73.11	474.83	49.45	93.7	−70.51
D1–D2	3.7	20.61	—	6.23	−0.65	6.28	−0.59	31.57	−0.07	6.51	−169
W1–W2	10.1	29.62	—	6.61	−0.44	6.75	−0.42	43	−0.44	6.07	−0.93

Notes: “W1–W2” means variable change from W1 to W2, and similarly for “D1–D2”. FRST—Forestland; PAST—Grassland; AGRL—Cropland; URHD—Urban land.

(1) Annual scale

The impacts of land-use change on annual sediment yield are shown in Figure 12 and Table 5. It is shown that when the baseline land use (consisting of cropland and forestland) was converted to cropland, the sediment yield increased 50.40% (61.36 tons). The scenarios of forestland (S1), grassland (S2) and urban land (S4) decreased the sediment yield by 72.96%, 72.60%, and 65.41% (89.57 tons, 89.16

tons, and 79.69 tons), respectively. The contribution of changes in individual land-use scenarios on sediment yield at annual scale was cropland > baseline > urban land > grassland > forestland.

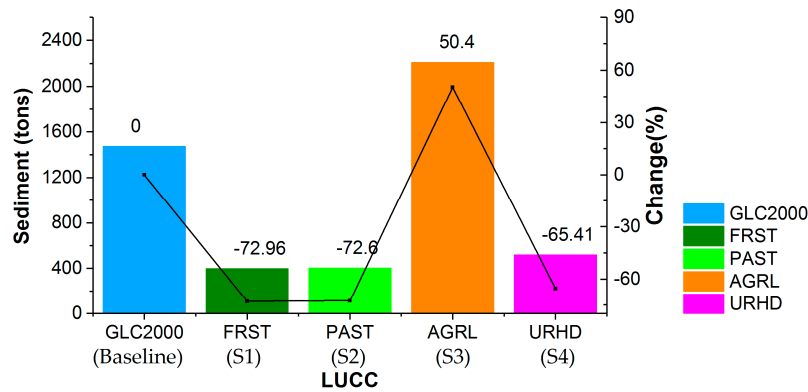


Figure 12. Responses of annual sediment yield to different land-use scenarios. Remarks: FRST—Forestland; PAST—Grassland; AGRL—Cropland; URHD—Urban land.

(2) Wet season and dry season

The effects of land-use change on sediment yield during the wet season (W1 and W2) were consistent to those at annual scale (Figure 13a,b). The change rates of sediment yield induced by different land-use scenarios during the W1 and W2 were nearly the same (Table 5). The urban land scenario (S4) during other statistical periods in this study typically decreased the sediment yield, while it produced substantial sediment (an increase of 139.32% (6.58 tons)) during D1, even more than cropland scenario (an increase of 53.29% (2.52 tons)) (Figure 13c and Table 5). The average reduction changes in sediment yield caused by forestland/grassland were approximately 73% and 69% during the wet and dry seasons, respectively. The contribution of changes in individual land-use scenarios on sediment yield during the wet season (W1 and W2) and D2 was cropland > baseline > urban land > grassland > forestland; however, it was urban land > cropland > baseline > grassland > forestland during D1.

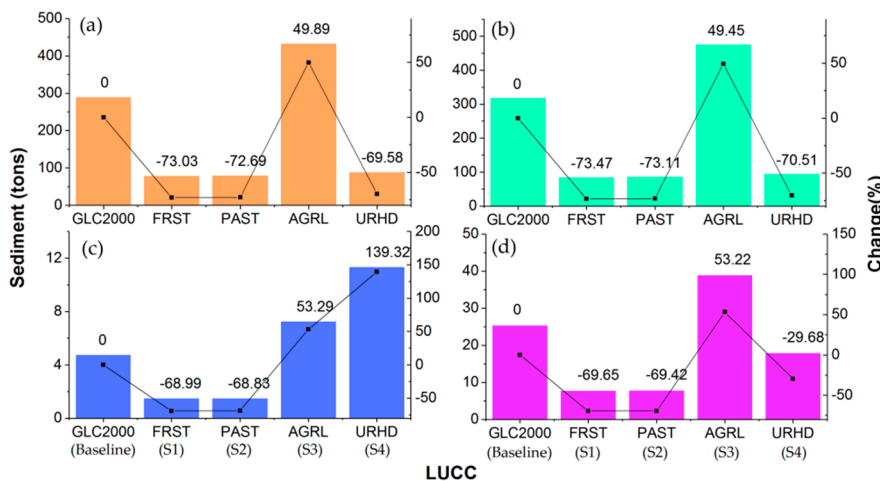


Figure 13. Sediment yield responses to different land-use scenarios during the wet season (W1 and W2) and dry season (D1 and D2): (a) refers to “W1”; (b) refers to “W2”; (c) refers to “D1”; and (d) refers to “D2”. FRST—Forestland; PAST—Grassland; AGRL—Cropland; URHD—Urban land.

4. Discussion

In this study, the CMADS + SWAT mode was used to calibrate and validate the runoff and sediment yield at monthly and daily scales. In general, satisfactory results have been achieved for monthly runoff, daily runoff, and monthly sediment yield. In the HRB, some studies in the upstream catchment area of the Dahuofang Reservoir using the SWAT model and driven by OBS have been conducted [39,62]. Compared with Han [39] and Yang [62], the CMADS + SWAT mode achieved a better result for monthly runoff and a worse but satisfactory result for monthly sediment yield. However, both of the researchers did not simulate runoff and sediment yield on the daily scale. In general, soil erosion is controlled by a variety of factors [6,37]. Regarding the sediment yield simulation, it tended to be underestimated during most summers. A similar phenomenon was shown in the Miyun Reservoir catchment [63]. In relatively extreme cases, high-speed surface runoff may cause strong erosion to the surface, and even landslides under the action of hydrodynamic force, resulting in a large amount of sediment transport in the river. However, there may be some uncertainties in the observed sediment data [64] for the model calibration and validation, although these data were obtained from authoritative reports issued by the Ministry of Water Resources of the P. R. China. Extraction techniques and sediment sampling intervals were not shown in the reports, and there were few monitoring points [64]. Thus, it is impossible to check whether sediment yield was underestimated or overestimated. Another possible reason for underestimating the sediment yield could be the limitations of the SCS-CN method. The duration and intensity of rainfall are not considered; instead, the average daily rainfall is used as a SWAT input [65]. In fact, high-intensity and even short-duration rainfall could generate more sediment than actualized in the model based on daily rainfall [63]. Overall, the CMADS can well reflect the climatic characteristics of the study area. The CMADS + SWAT mode is reliable and CMADS can be used for other studies in the HRB.

The runoff responses under each land-use scenario at the dry seasonal scale were different from that at annual and wet seasonal scales (Table 4); while the sediment yield responses under each land-use scenario were similar at annual and seasonal scales (Table 5). At annual and wet seasonal scales, the scenarios of forestland (S1) and grassland (S2) increased percolation loss to depth, decrease WYLD, and lead to decrease in runoff. However, it was the opposite during the dry season. Deforestation and urbanization usually decrease ET and percolation, increase WYLD and SURQ, and lead to increase in runoff [14,37]. Guo et al. [66] reported that the increase in forest cover, due to the conversion of agricultural lands to forest, reduced runoff in the wet season but increased it in the dry season in the Poyang Lake basin. Fu et al. [67] found that in Northeastern China, the conversion of cropland, forestland, and grassland into forestland/grassland resulted in the reduction of the monthly runoff from March to August, while the runoff for other months increased; however, the situation was the opposite when the cropland, forestland, and grassland were converted into croplands. The change ratios for the forestland scenario (from -13.83% to 20.03%) and grassland scenario (from -11.27% to 2.57%) (Table 4) showed that forestland had a greater advantage than grassland in reducing flood potentials during the wet season and in moderating drought severity during the dry season. A similar pattern of runoff responses was noted by Lin et al. [14] and Guo et al. [66]. In contrast, Huang et al. [68] found that the forestland was no better than grassland in conserving water when the canopy cover of forestland was less than grassland; we also noticed that some studies found the forest changes has limited [69] or no influence [70] on watershed flows of rivers. In addition, forestland was expected to greatly reduce flood for small storms but less significance for the largest storms [71]. As shown in Table 4, when the rainfall was large, the hydrological changes could be weakened due to land-use change. Because of the retention effect of forests on floods, the remaining water flow may overlap with the latter flood peaks, thus causing greater disasters than that of nonforestland, if the previous flood outflow process was not over yet and a new storm occurred [72]. In this study, the precipitation was 246.27 mm, but runoff yield was 264.62 mm in the Beikouqian region (almost covered by forestland) during August 2013. It might be the overlapping of flood peaks that resulted in an extraordinary flood disaster. The urban land, covered by many impervious layers, usually significantly decreased ET,

SW, PERC, and GW_Q, and increased SURQ and WYLD, leading to a relative significant increase in runoff. Similar conclusions have been drawn by many studies [34,65,73]. Chang et al. [74] indicated that only the urban watershed exhibited a significant increase in both wet and dry season runoff ratios. In fact, because the runoff generated by urban land is closely related to precipitation, it was less than that of forestland in the early dry season (September to November) (Figure 10). In all the statistical periods, both forestland (S1) and grassland (S2) scenarios reduced sediment yield by approximately 70%, while sediment yield increased by about 50% under cropland scenario (S3). Forestland and grassland can protect soil from erosion, while cropland generated more sediment [6]. Yan et al. [37] reported that cropland (forestland) had a greater positive (negative) effect on sediment yield, with negative regression coefficients between grassland and urban land and the sediment yield in the Upper Du Watershed. Serpa et al. [53] found the cropland depicted the highest erosion rates, and forests typically had lower erosion rates than grasslands. Urban land scenario (S4) decreased sediment yield by more than 60% at annual and wet seasonal scales. However, sediment yield reduced by 29.68% in D1 while it increased by 139.32% (the change rate even more than cropland scenario) in D2. The primary reason for this might be that the urban land scenario (S4) is prone to produce more runoff than cropland scenario (S3) in D1, leading to higher sediment transport to the rivers (Figures 11c and 13c). However, when the precipitation is no longer a factor restricting the runoff caused by cropland, more sediment will be produced by the cropland (Table 5). Moreover, heavy rainfall can weaken the hydrological processes such as interception and infiltration of the underlying surface (Table 4) [14], as well as the influence of underlying surface conditions on the relationship between rainfall and sediment yield (Table 5) [75].

In this study, we only investigated the effects of land-use change (LUCC only occurred in the downstream of the BRB) on runoff and sediment yield at annual and seasonal (W1, W2, D1, and D2) scales. However, we noticed many studies have demonstrated that runoff and sediment transport processes can be significantly influenced by the spatial distribution patterns of land use at different temporal and spatial scales. Yin et al. [76] reported that the impacts of LUCC changes on flow regimes were greater after the “Grain for Green Program” in the downstream areas of the Jinghe River Basin than in the upstream. Lin et al. [14] analyzed the land-use change impacts on catchment runoff using different time indicators and the results showed a varying change in runoff among three time scales and three catchments. Khoi et al. [6] compared their results to several studies in Vietnam and found that a smaller change because of LUCC occurred in streamflow and sediment yield, which could be explained by the approximately 50% change in forest land that occurred in the downstream. Interestingly, in our study, although the LUCC only occurred in the downstream of the BRB, significant change ratios were predicted for runoff and sediment yield under individual land-use scenarios at annual and seasonal scales. Although the area of BRB is small, the effects of individual land-use types on runoff and sediment yield at annual and seasonal scales were relatively clearly shown. Due to the heterogeneity in landscape, climate, and geology in the watersheds, it is essential to quantify the effects of spatial distribution patterns of land use for a local scale. Our further work will analyze the impact of land-use pattern changes on runoff and sediment in the HRB from the perspective of large-scale and multi-time.

Undeniably speaking, the SWAT model is useful and effective to investigate the responses of runoff and sediment yield to land-use change, but some limitations as well as uncertainties exist in both the data and the model. The runoff and sediment yield may be influenced by the resolution of the DEM, soil, and land use and the watershed and HRU delineation [77]. Precipitation is a key factor affecting runoff events and sediment exports [78,79], whereas precipitation is adopted in each sub-basin in a basin according to the nearest rain gauge to the sub-basin centroid [80]. Therefore, having a good number and distribution of rain gauges in a basin is very beneficial for simulations of hydrological processes. In this study, ten CMADS stations selected by SWAT were relatively uniform distribution in the HRB (Figure 1). Acceptable and relatively stable model performance was achieved when the rain gauge density ranged between 1.0 and 1.4 per 1000 km² [81], and the station density was 1.26 per 1000 km² in the HRB. Moreover, a number of empirical and quasiphysical equations in SWAT

model were developed based on climatic conditions in the U.S., which may not be appropriate for the climate in China, such as the SCS-CN method and MUSLE method [82]. The MUSLE method does not include the processes occurring in the watershed for both erosions caused by landslides and the “second-storm effect” effecting the mobilization of particulates from soil surface [83]. This may lead to great effects on the results for sediment yield simulations, especially at daily scale. The databases in SWAT were also mostly developed to reflect North American conditions, while the transferability of that to Chinese conditions is doubted by Ongley et al. [84]. It is suggested that some parameters in the empirical equations and the SWAT databases should be modified to suit Chinese conditions in order to improve the simulation results. In addition, calibrated parameters are conditioned on the choice of objective function, the type and length of measured data, and the procedure used for calibration, etc. [55]. Of course, the accuracy of the data is necessary for model simulation. Despite these limitations and uncertainties, the simulation results for monthly/daily runoff and monthly sediment yield were satisfactory according to Moriasi et al. [56].

5. Conclusions

In this research, the SWAT model driven by the CMADS was successfully applied to the HRB, specifically to determine the monthly and daily runoffs. Because many factors can affect the calibration and verification of sediment yield, the simulations of sediment yield in this study were not perfect, but the production of monthly sediment was simulated to meet the requirements (2014 selected as the validation period). The results demonstrated that CMADS was a reliable meteorological data source for the HRB, and the model application was a valid tool for investigating the impacts of land-use changes on runoff and sediment yield. CMADS has been successfully applied in some areas of China and other East Asian countries (e.g., South Korea), and can reflect the climatic characteristics of these areas well, perhaps providing valuable meteorological data for the regions with scarce gauge stations. Moreover, CMADS can be further improved its accuracy of data in other East Asian countries through revising by local measured data. CMADS covered only nine years (2008–2016); if the time series could be extended for decades, it may help researchers to conduct more extensive research in East Asia.

At the sub-basin scale (BRB), the responses of individual land-use types to annual and seasonal runoff and sediment yield using scenario assumptions were determined. Our research indicated that the effects of land-use type on water balance components, runoff, and sediment yield might be altered when different time scales were considered. The changes of water balance components, runoff, and sediment yield under individual land-use scenarios were similar between the annual and wet seasonal scale. Compared with grassland, forestland played a more active role in water redistribution from the wet season to the dry season by promoting infiltration-recharging-discharging processes, and in reducing the soil erosion. However, during the wet season, forestland may lead to greater flood disaster when the subsurface water flow overlaps with the latter flood peaks, because more water is stored in soil and bedrock in forestland. Deforestation and urbanization usually reduce evapotranspiration and water penetration, and increase SURQ, thereby leading to an increase in runoff. Relatively lower runoff occurred under the cropland and urban land scenarios in the early dry season, because the water stored by grassland and forestland during the wet season recharged the river flow, particularly for forestland. Cropland, due to high soil erosion, increased the amount of sediment to be transported into the river along with runoff. On the other hand, under light precipitation (or runoff) conditions, urban land might increase sediment export more, resulting from a relatively larger runoff. In addition, heavy rainfall can weaken the hydrological processes such as interception and infiltration of the underlying surface, as well as the influence of underlying surface conditions on the relationship between rainfall and sediment yield. The limitations as well as uncertainties in SWAT may influence the results in terms of runoff and sediment yield simulations. In general, this study provides useful information for policy makers about the influences of each land-use type on soil and water conservation at annual and

seasonal scales in the HRB during urbanization. The influence of land-use pattern change on runoff and sediment yield in river basins needs to be further studied.

Author Contributions: The modeling and writing of this work by L.Z.; X.M. designed the experiments; Observed data was provided by X.M. and M.Y.; the improvement of manuscript writing by X.M. and H.W.

Funding: This research was financially joint supported by the National Science Foundation of China (41701076); the National key Technology R & D Program of China (2017YFC0404305); Young Elite Scientists Sponsorship Program by CAST (2017QNRC001); National Science Foundation for Young Scientists of China (Grant No.51709271).

Conflicts of Interest: The authors declare no conflict of interest.

References

- Armanini, D.G.; Horrigan, N.; Monk, W.A.; Peters, D.L.; Baird, D.J. Development of a benthic macroinvertebrate flow sensitivity index for Canadian rivers. *River Res. Appl.* **2011**, *27*, 723–737. [[CrossRef](#)]
- Piao, S.L.; Ciais, P.; Huang, Y.; Shen, Z.H.; Peng, S.S.; Li, J.S.; Zhou, L.P.; Liu, H.Y.; Ma, Y.C.; Ding, Y.H.; et al. The impacts of climate change on water resources and agriculture in China. *Nature* **2010**, *467*, 43–51. [[CrossRef](#)] [[PubMed](#)]
- Notter, B.; Hurni, H.; Wiesmann, U.; Abbaspour, K.C. Modelling water provision as an ecosystem service in a large East African river basin. *Hydrol. Earth Syst. Sci.* **2012**, *16*, 69–86. [[CrossRef](#)]
- Wolka, K.; Mengistu, T.; Taddese, H.; Tolera, A. Impact of Land Cover Change on Water Quality and Stream Flow in Lake Hawassa Watershed of Ethiopia. *Agric. Sci.* **2014**, *5*, 647–659. [[CrossRef](#)]
- Zhang, M.F.; Liu, N.; Harper, R.; Li, Q.; Liu, K.; Wei, X.; Ning, D.Y.; Hou, Y.P.; Liu, S.R. A global review on hydrological responses to forest change across multiple spatial scales: Importance of scale, climate, forest type and hydrological regime. *J. Hydrol.* **2017**, *546*, 44–59. [[CrossRef](#)]
- Khoi, D.N.; Suetsugi, T. The responses of hydrological processes and sediment yield to land-use and climate change in the Be River Catchment, Vietnam. *Hydrol. Process.* **2014**, *28*, 640–652. [[CrossRef](#)]
- Li, Z.; Liu, W.Z.; Zhang, X.C.; Zheng, F.L. Impacts of land use change and climate variability on hydrology in an agricultural catchment on the Loess Plateau of China. *J. Hydrol.* **2009**, *377*, 35–42. [[CrossRef](#)]
- Nunes, J.P.; Naranjo Quintanilla, P.; Santos, J.M.; Serpa, D.; Carvalho-Santos, C.; Rocha, J.; Keizer, J.J.; Keesstra, S.D. Afforestation, subsequent forest fires and provision of hydrological services: A model-based analysis for a Mediterranean mountainous catchment. *Land Degrad. Dev.* **2018**, *29*, 776–788. [[CrossRef](#)]
- Ghaffari, G.; Keesstra, S.; Ghodousi, J.; Ahmadi, H. SWAT-simulated hydrological impact of land-use change in the Zanjanrood basin, Northwest Iran. *Hydrol. Process.* **2010**, *24*, 892–903. [[CrossRef](#)]
- Cerdan, O.; Govers, G.; Le Bissonnais, Y.; Van Oost, K.; Poesen, J.; Saby, N.; Gobin, A.; Vacca, A.; Quinton, J.; Auerswald, K.; et al. Rates and spatial variations of soil erosion in Europe: A study based on erosion plot data. *Geomorphology* **2010**, *122*, 167–177. [[CrossRef](#)]
- García-Ruiz, J.M. The effects of land uses on soil erosion in Spain: A review. *Catena* **2010**, *81*, 1–11. [[CrossRef](#)]
- Keesstra, S.D. Impact of natural reforestation on floodplain sedimentation in the Dragonja basin, SW Slovenia. *Earth Surf. Process. Landf.* **2007**, *32*, 49–65. [[CrossRef](#)]
- Buendia, C.; Bussi, G.; Tuset, J.; Vericat, D.; Sabater, S.; Palaub, A.; Batalla, R.J. Effects of afforestation on runoff and sediment load in an upland Mediterranean catchment. *Sci. Total Environ.* **2016**, *540*, 144–157. [[CrossRef](#)]
- Lin, B.Q.; Chen, X.W.; Yao, H.X.; Chen, Y.; Liu, M.B.; Gao, L.; James, A. Analyses of landuse change impacts on catchment runoff using different time indicators based on SWAT model. *Ecol. Indic.* **2015**, *58*, 55–63. [[CrossRef](#)]
- Mueller, E.N.; Francke, T.; Batalla, R.J.; Bronstert, A. Modelling the effects of land-use change on runoff and sediment yield for a meso-scale catchment in the Southern Pyrenees. *Catena* **2009**, *79*, 288–296. [[CrossRef](#)]
- Zhan, C.S.; Jiang, S.S.; Sun, F.B.; Jia, Y.W.; Yue, W.F.; Niu, C.W. Quantitative contribution of climate change and human activities to runoff changes in the Wei River basin, China. *Hydrol. Earth Syst. Sci.* **2014**, *18*, 3069–3077. [[CrossRef](#)]
- Li, H.Y.; Zhang, Y.Q.; Vaze, J.; Wang, B.D. Separating effects of vegetation change and climate variability using hydrological modeling and sensitivity-based approaches. *J. Hydrol.* **2012**, *420*, 403–418. [[CrossRef](#)]

18. Lørup, J.K.; Refsgaard, J.C.; Mazvimavi, D. Assessing the effect of land use change on catchment runoff by combined use of statistical tests and hydrological modelling: Case studies from Zimbabwe. *J. Hydrol.* **1998**, *205*, 147–163. [[CrossRef](#)]
19. Wei, X.H.; Li, W.H.; Zhou, G.Y.; Liu, S.R.; Sun, G. Forests and Streamflow—Consistence and Complexity. *J. Nat. Resour.* **2005**, *20*, 761–770.
20. Yao, Y.L.; Lu, X.G.; Wang, L. A Review on Study Methods of Effect of Land Use and Cover Change on Watershed Hydrology. *Wetl. Sci.* **2009**, *7*, 83–88.
21. Arnold, J.G.; Srinivasan, R.; Muttiah, R.S.; Williams, J.R. Large area hydrologic modeling and assessment. Part I: Model development. *J. Am. Water Resour. Assoc.* **1998**, *34*, 73–89. [[CrossRef](#)]
22. SWAT Literature Database. Available online: https://www.card.iastate.edu/swat_articles/ (accessed on 15 July 2018).
23. SWAT Official Website. Available online: <https://swat.tamu.edu/> (accessed on 21 May 2018).
24. Gassman, P.W.; Sadeghi, A.M.; Srinivasan, R. Applications of the SWAT Model Special Section: Overview and Insights. *J. Environ. Qual.* **2014**, *43*, 1–8. [[CrossRef](#)]
25. Abbaspour, K.C.; Yang, J.; Maximov, I.; Siber, R.; Bogner, K.; Mieleitner, J.; Zobrist, J.; Srinivasan, R. Modelling hydrology and water quality in the pre-alpine/alpine Thur watershed using SWAT. *J. Hydrol.* **2007**, *333*, 413–430. [[CrossRef](#)]
26. Meng, X.; Wang, H.; Shi, C.; Wu, Y.; Ji, X. Establishment and Evaluation of the China Meteorological Assimilation Driving Datasets for the SWAT Model (CMADS). *Water* **2018**, *10*, 1555. [[CrossRef](#)]
27. Meng, X.; Wang, H.; Wu, Y.P.; Long, A.H.; Wang, J.H.; Shi, C.X.; Ji, X.N. Investigating spatiotemporal changes of the land-surface processes in Xinjiang using high-resolution CLM3.5 and CLDAS: Soil temperature. *Sci. Rep.* **2017**, *7*, 13286. [[CrossRef](#)]
28. Meng, X.; Wang, H.; Lei, X.H.; Cai, S.Y.; Wu, H.J.; Ji, X.N.; Wang, J.H. Hydrological Modeling in the Manas River Basin Using Soil and Water Assessment Tool Driven by CMADS. *Teh. Vjesn.* **2017**, *24*, 525–534. [[CrossRef](#)]
29. Liu, J.; Shangguan, D.; Liu, S.; Ding, Y. Evaluation and Hydrological Simulation of CMADS and CFSR Reanalysis Datasets in the Qinghai-Tibet Plateau. *Water* **2018**, *10*, 513. [[CrossRef](#)]
30. Meng, X.; Wang, H. Significance of the China Meteorological Assimilation Driving Datasets for the SWAT Model (CMADS) of East Asia. *Water* **2017**, *9*, 765. [[CrossRef](#)]
31. Shao, G.; Guan, Y.; Zhang, D.; Yu, B.; Zhu, J. The Impacts of Climate Variability and Land Use Change on Streamflow in the Hailiutu River Basin. *Water* **2018**, *10*, 814. [[CrossRef](#)]
32. Thom, V.; Li, L.; Jun, K.S. Evaluation of Multi-Satellite Precipitation Products for Streamflow Simulations: A Case Study for the Han River Basin in the Korean Peninsula, East Asia. *Water* **2018**, *10*, 642. [[CrossRef](#)]
33. Cao, Y.; Zhang, J.; Yang, M.; Lei, X.; Guo, B.; Yang, L.; Zeng, Z.; Qu, J. Application of SWAT Model with CMADS Data to Estimate Hydrological Elements and Parameter Uncertainty Based on SUFI-2 Algorithm in the Lijiang River Basin, China. *Water* **2018**, *10*, 742. [[CrossRef](#)]
34. Dong, N.P.; Yang, M.X.; Meng, X.Y.; Liu, X.; Wang, Z.; Wang, H.; Yang, C. CMADS-Driven Simulation and Analysis of Reservoir Impacts on the Streamflow with a Simple Statistical Approach. *Water* **2018**, *11*, 178. [[CrossRef](#)]
35. Yuan, Z.; Xu, J.; Meng, X.; Wang, Y.; Yan, B.; Hong, X. Impact of Climate Variability on Blue and Green Water Flows in the Erhai Lake Basin of Southwest China. *Water* **2019**, *11*, 424. [[CrossRef](#)]
36. Meng, X.; Wang, H.; Chen, J. Profound Impacts of the China Meteorological Assimilation Driving Datasets for the SWAT Model (CMADS). *Water* **2019**, *11*, 832. [[CrossRef](#)]
37. Yan, B.; Fang, N.F.; Zhang, P.C.; Shi, Z.H. Impacts of land use change on watershed streamflow and sediment yield: An assessment using hydrologic modelling and partial least squares regression. *J. Hydrol.* **2013**, *484*, 26–37. [[CrossRef](#)]
38. Qiu, L.; Wu, Y.; Wang, L.; Lei, X.; Liao, W.; Hui, Y.; Meng, X. Spatiotemporal response of the water cycle to land use conversions in a typical hilly-gully basin on the Loess Plateau, China. *Hydrol. Earth Syst. Sci.* **2017**, *21*, 6485–6499. [[CrossRef](#)]
39. Han, C.W. *Environmental Behavior, Simulation and Prediction of Nonpoint Source Nitrogen and Phosphorus in Cold Regions*; Dalian University of Technology: Dalian, China, 2011.
40. Liu, Y. *Research on Water Pollution Control Planning in Shenfu New Town*; Shenyang Jianzhu University: Shenyang, China, 2013.

41. DEM Derived from CGIAR-CSI. Available online: <http://srtm.csi.cgiar.org/SELECTION/inputCoord.asp> (accessed on 16 June 2018).
42. China Soil Map Based Harmonized World Soil Database (v1.1). Available online: <http://westdc.westgis.ac.cn> (accessed on 20 June 2018).
43. Fischer, G.; Nachtergaele, F.; Prieler, S.; Velthuisen, H.T.; Verelst, L.; Wiberg, D. *Global Agro-ecological Zones Assessment for Agriculture (GAEZ 2008)*; IIASA: Laxenburg, Austria; FAO: Rome, Italy, 2008.
44. Saxton, K.E.; Rawls, W.J. Soil water characteristic estimates by texture and organic matter for hydrologic solutions. *Soil Sci. Soc. Am. J.* **2006**, *70*, 1569–1578. [[CrossRef](#)]
45. Ran, Y.H.; Li, X.; Lu, L. Evaluation of four remote sensing based land cover products over China. *Int. J. Remote Sens.* **2010**, *31*, 391–401. [[CrossRef](#)]
46. Arnold, J.G.; Moriasi, D.N.; Gassman, P.W.; Abbaspour, K.C.; White, M.J.; Srinivasan, R.; Santhi, C.; Harmel, D.; van Griensven, A.; Van Liew, M.W.; et al. SWAT: Model use, calibration, and validation. *Trans. ASABE* **2012**, *55*, 1491–1508. [[CrossRef](#)]
47. Arnold, J.G.; Allen, P.M. Estimating hydrologic budgets for three Illinois watersheds. *J. Hydrol.* **1996**, *176*, 57–77. [[CrossRef](#)]
48. Luo, K.S.; Tao, F.L.; Moiwo, J.P.; Xiao, D.P. Attribution of hydrological change in Heihe River Basin to climate and land use change in the past three decades. *Sci. Rep.* **2016**, *6*, 33704. [[CrossRef](#)]
49. USDA Soil Conservation Service. *National Engineering Handbook Section 4 Hydrology*; USDA-Soil Conservation Service: Washington, DC, USA, 1972; Chapters 4–10.
50. Monteith, J.L. Evaporation and the Environment in the State and Movement of Water in Living Organisms. In *Proceedings of the 19th Symposia of the Society for Experimental Biology*; Cambridge University Press: London, UK, 1965; pp. 205–234.
51. Williams, J.R. Flood routing with variable travel time or variable storage coefficients. *Trans. ASAE* **1969**, *12*, 100–103. [[CrossRef](#)]
52. Williams, J.R.; Berndt, H.D. Sediment Yield Prediction Based on Watershed Hydrology. *Trans. ASAE* **1977**, *20*, 1100–1104. [[CrossRef](#)]
53. Serpa, D.; Nunes, J.P.; Santos, E.S.; Jacinto, R.; Veiga, S.; Lima, J.C.; Moreira, M.; Corte-Real, J.; Keizer, J.J.; Abrantes, N. Impacts of climate and land use changes on the hydrological and erosion processes of two contrasting Mediterranean catchments. *Sci. Total Environ.* **2015**, *538*, 64–77. [[CrossRef](#)]
54. Faramarzi, M.; Abbaspour, K.C.; Schulin, R.; Yang, H. Modelling blue and green water resources availability in Iran. *Hydrol. Process.* **2009**, *23*, 486–501. [[CrossRef](#)]
55. Yang, J.; Reicher, P.; Abbaspour, K.C.; Xia, J.; Yang, H. Comparing uncertainty analysis techniques for a SWAT Application to the Chaohe Basin in China. *J. Hydrol.* **2008**, *58*, 1–23. [[CrossRef](#)]
56. Moriasi, D.N.; Arnold, J.G.; Van Liew, M.W.; Bingner, R.L.; Harmel, R.D.; Veith, T.L. Model evaluation guidelines for systematic quantification of accuracy in watershed simulations. *Am. Soc. Agric. Biol. Eng.* **2007**, *50*, 885–900. [[CrossRef](#)]
57. Santhi, C.; Arnold, J.G.; Williams, J.R.; Dugas, W.A.; Srinivasan, R.; Hauck, L.M. Validation of the SWAT model on a large river basin with point and nonpoint sources. *J. Am. Water Resour. Assoc.* **2001**, *37*, 1169–1188. [[CrossRef](#)]
58. Garbrecht, J.D.; Van Liew, M.W.; Arnold, J.G. Hydrologic simulation on agricultural watersheds: Choosing between two models. *Trans. ASAE* **2003**, *46*, 1539–1551. [[CrossRef](#)]
59. 2013 Bulletin of Flood and Drought Disaster in China. Available online: http://www.mwr.gov.cn/sj/tjgb/zgshzhgb/201612/t20161222_776091.html (accessed on 2 July 2018).
60. Zhang, P. *Study on Risk Assessment and Prevention of Huangdai Gully Debris Flow in Changsha Village, Qingyuan Country*; Jilin University: Changchun, China, 2017.
61. Bieger, K.; Hormann, G.; Fohrer, N. Simulation of Streamflow and Sediment with the Soil and Water Assessment Tool in a Data Scarce Catchment in the Three Gorges Region, China. *J. Environ. Qual.* **2014**, *43*, 37–45. [[CrossRef](#)]
62. Yang, W. *Simulation on Agricultural Non-Point Sources Pollution and Risk Assessment in Dahuofang Reservoir Catchment of Liaoning Province*; Jilin University: Changchun, China, 2012.
63. Xu, Z.X.; Pang, J.P.; Liu, C.M.; Li, J.Y. Assessment of runoff and sediment yield in the Miyun Reservoir catchment by using SWAT model. *Hydrol. Process.* **2009**, *23*, 3619–3630. [[CrossRef](#)]

64. Wang, S.; Luan, J.; Liu, Q. Analysis of Sediment Characteristics in Upper Hunhe River Basin (Fushun Section). *Water Resour. Hydr. Northeast. Chin.* **2008**, *26*, 28–29.
65. Nie, W.M.; Yuan, Y.P.; Kepner, W.; Nash, M.S.; Jackson, M.; Erickson, C. Assessing impacts of landuse changes on hydrology for the upper San Pedro watershed. *J. Hydrol.* **2011**, *407*, 105–114. [[CrossRef](#)]
66. Guo, H.; Hu, Q.; Jiang, T. Annual and seasonal streamflow responses to climate and land-cover changes in the Poyang Lake basin, China. *J. Hydrol.* **2008**, *355*, 106–122. [[CrossRef](#)]
67. Fu, Q.; Shi, R.; Li, T.; Sun, Y.; Liu, D.; Cui, S.; Hou, R. Effects of land-use change and climate variability on streamflow in the Woken River basin in Northeast China. *River Res. Appl.* **2019**, *35*, 121–132. [[CrossRef](#)]
68. Huang, M.B.; Kang, S.Z.; Li, Y.S. A comparison of hydrological behavior of forest and grassland watersheds in gully region of the Loess Plateau. *J. Nat. Resour.* **1999**, *14*, 226–231.
69. Buttle, J.M.; Metcalfe, R.A. Boreal forest disturbance and streamflow response, northeastern OntarioCan. *J. Fish. Aquat. Sci.* **2000**, *57*, 5–18. [[CrossRef](#)]
70. Ceballos-Barbancho, A.; Morán-Tejeda, E.; Luengo-Ugidos, M.A.; Llorente-Pinto, J.M. Water resources and environmental change in a Mediterranean environment: The south-west sector of the Duero river basin (Spain). *J. Hydrol.* **2008**, *351*, 126–138. [[CrossRef](#)]
71. Calder. *Land Use Impacts on Water Resources. Land-Water Linkages in Rural Watersheds Electronic Workshop*; FAO: Rome, Italy, 2000.
72. Sun, H. Progress of the research on the role of the forest during the past 20 years. *J. Nat. Resour.* **2001**, *16*, 407–412.
73. Wang, Y.; Qi, S.; Sun, G.; Steve, G. Impacts of climate and land-use change on water resources in a watershed: A case study on the Trent River basin in North Carolina, USA. *Adv. Water Sci.* **2011**, *22*, 51–58.
74. Chang, H. Comparative streamflow characteristics in urbanizing basins in the Portland Metropolitan Area, Oregon, USA. *Hydrol. Process.* **2007**, *21*, 211–222. [[CrossRef](#)]
75. Hao, F.; Chen, L.; Liu, C.; Dai, D. Impact of Land Use Change on Runoff and Sediment Yield. *J. Soil Water Conserv.* **2004**, *18*, 5–8.
76. Yin, J.; He, F.; Xiong, Y.J.; Qiu, G.Y. Effects of land use/land cover and climate changes on surface runoff in a semi-humid and semi-arid transition zone in northwest China. *Hydrol. Earth Syst. Sci.* **2017**, *21*, 183–196. [[CrossRef](#)]
77. Gassman, P.W.; Reyes, M.R.; Green, C.H.; Arnold, J.G. The Soil and Water Assessment Tool: Historical development, applications, and future research directions. *Trans. ASABE* **2007**, *50*, 1211–1240. [[CrossRef](#)]
78. Keesstra, S.D.; Davis, J.; Masselink, R.H.; Casalí, J.; Peeters, E.T.; Dijkma, R. Coupling hysteresis analysis with sediment and hydrological connectivity in three agricultural catchments in Navarre, Spain. *J. Soil. Sediment.* **2019**, *19*, 1598–1612. [[CrossRef](#)]
79. Masselink, R.H.; Temme, A.J.A.M.; Giménez Díaz, R.; Casalí Sarasíbar, J.; Keesstra, S.D. Assessing hillslope-channel connectivity in an agricultural catchment using rare-earth oxide tracers and random forests models. *Cuad. Investig. Geogr.* **2017**, *43*, 19–39. [[CrossRef](#)]
80. Douglas-Mankin, K.R.; Srinivasan, R.; Arnold, A.J. Soil and Water Assessment Tool (SWAT) Model: Current Developments and Applications. *Trans. ASABE* **2010**, *53*, 1423–1431. [[CrossRef](#)]
81. Xu, H.; Xu, C.Y.; Chen, H.; Zhang, Z.; Li, L. Assessing the influence of rain gauge density and distribution on hydrological model performance in a humid region of China. *J. Hydrol.* **2013**, *505*, 1–12. [[CrossRef](#)]
82. Neitsch, S.L.; Arnold, J.G.; Kiniry, J.R.; Williams, J.R. *Soil and Water Assessment Tool Theoretical Documentation Version 2009*; Texas Water Resources Institute: College Station, TX, USA, 2011.
83. Abbaspour, K.C. *SWAT-CUP: SWAT Calibration and Uncertainty Programs—A User Manual (Version 2012)*; Swiss Federal Institute of Aquatic Science and Technology: Dübendorf, Switzerland, 2011.
84. Ongley, E.D.; Zhang, X.; Yu, T. Current status of agricultural and rural non-point source pollution assessment in China. *Environ. Pollut.* **2010**, *158*, 1159–1168. [[CrossRef](#)]

